Exploiting Nonclassical Motion of a Trapped Ion Crystal for Quantum-Enhanced Metrology of Global and Differential Spin Rotations

R. J. Lewis-Swan,[1,2] J. C. Zuñiga Castro,[1,2] D. Barberena,[3,4] and A. M. Rey[3,4]

[1]*Homer L. Dodge Department of Physics and Astronomy, The University of Oklahoma, Norman, Oklahoma 73019, USA*

[2]*Center for Quantum Research and Technology, The University of Oklahoma, Norman, Oklahoma 73019, USA*

[3]*JILA, NIST, and Department of Physics, University of Colorado, Boulder, Colorado, USA*

[4]*Center for Theory of Quantum Matter, University of Colorado, Boulder, Colorado, USA*

(Received 4 December 2023; revised 23 February 2024; accepted 18 March 2024; published 15 April 2024)

We theoretically investigate prospects for the creation of nonclassical spin states in trapped ion arrays by coupling to a squeezed state of the collective motion of the ions. The correlations of the generated spin states can be tailored for quantum-enhanced sensing of global or differential rotations of subensembles of the spins by working with specific vibrational modes of the ion array. We propose a pair of protocols to utilize the generated states and demonstrate their viability even for small systems, while assessing limitations imposed by spin-motion entanglement and technical noise. Our work suggests new opportunities for the preparation of many-body states with tailored correlations for quantum-enhanced metrology in spin-boson systems.

DOI: 10.1103/PhysRevLett.132.163601

Introduction.—Preparing entangled atomic states is a continuing challenge for the realization of quantum-enhanced sensors. A strong focus has been on generating collective states as these are optimal for applications that include atomic clocks and interferometers [1,2]. However, recent work has drawn attention to the engineering of states with distributed entanglement and correlations for multiparameter estimation or quantum sensors with enhanced spatial resolution [3–10].

One way to prepare collective entangled states is to realize global spin-spin interactions mediated by a common bosonic mode uniformly coupled to a spin ensemble, such as in trapped ion [11,12] and cavity-QED [13–15] platforms. In the former, squeezed states—featuring a reduction in quantum projection noise for specific observables—have been realized in both one-dimensional (1D) [16] and two-dimensional (2D) ion arrays [17]. However, the requirement to operate in a far-detuned regime can lead to challenges such as slow timescales for entangling dynamics relative to intrinsic decoherence, and spurious couplings to other boson modes that lead to a reduction in the effective range of spin-spin interactions. Both issues limit the amount of squeezing that can be generated.

Concurrently, the trapped ion community has made strides forward in the coherent control of the quantized vibrational motion of the ions for quantum information processing, simulation, and logic spectroscopy [18–25]. In this light, we investigate the feasibility of creating entangled spin states through coherent transfer of squeezed fluctuations from the motional to the spin degree of freedom, which builds on early ideas to generate squeezing with trapped ions [26,27] and demonstrated in atom-light systems [28,29].

Our proposal to use a resonant spin-boson coupling with a single mode leads to states featuring squeezing of a fixed spin quadrature and a coherent transfer time that is independent of the degree of the initial squeezing. Moreover, we show that spatially inhomogeneous spin-boson couplings can be used to create spin states with enhanced sensitivity to differential rotations between two parts of the array. The latter capability can have potential applications for clock comparisons [30,31], gravitational redshift measurements [32], or magnetometry [33]. The generated states can enable quantum-enhanced Ramsey interferometry even for small numbers of ions, relevant for near-term experiments, with performance that is fundamentally constrained by the buildup of spin-motion entanglement. To overcome this issue, and exploit the generated squeezing without the need for site-resolved measurements, we propose an interaction-based readout (IBR) protocol based on time-reversed dynamics [34–38] that disentangles the degrees of freedom and requires only global manipulations and measurements of the spins.

Spin-boson toolkit.—We consider a linear chain of N ions with $m = 1, 2, \ldots, N$ axial phonon modes with harmonic frequencies ω_m and associated bosonic creation (annihilation) operators $\hat{a}_m^\dagger$ ($\hat{a}_m$). We focus on axial motion in 1D for simplicity, but it is straightforward to extend our analysis to radial modes or higher dimensional arrays. A spin-1/2 is encoded in a pair of internal states $|\downarrow\rangle$ and $|\uparrow\rangle$ of each ion. State-of-the-art trapped ion quantum simulators provide a toolbox of operations to manipulate and couple spin and motion.

Global spin rotations are realized by driving the qubits with optical or microwave fields. The phonons can be

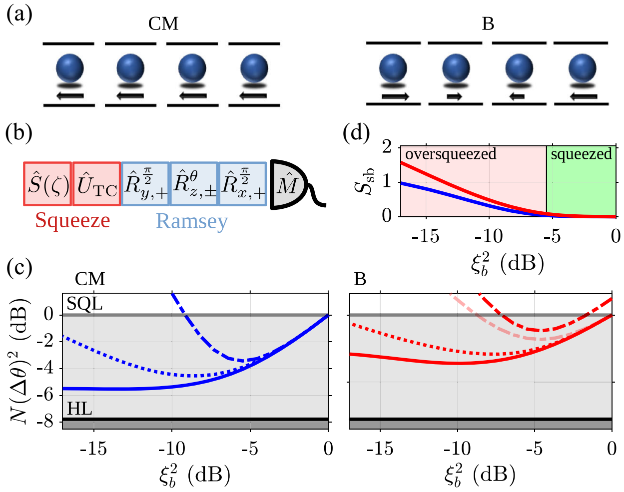

FIG. 1. (a) Example modes of a 1D chain. Arrows qualitatively indicate the ion participation in each mode. (b) Sequence for NR protocol. (c) Metrological gain $N(\Delta\theta)^2$ as a function of boson squeezing ξ_b^2. The performance achieved with measurements of $\hat{M} = \hat{S}_{z,+}$ (CM, dot-dashed line), $\hat{\mathcal{S}}_z$ (B, dot-dashed line) and $\hat{S}_{z,-}$ (B, faded dot-dashed line) is compared to the QCRB given by the QFI of the full system, $N(\Delta\theta)^2 = N/F_Q$ (solid lines). We also compare against the spin-only QFI via $N/F_{Q,s}$ (dotted lines). (d) Spin-boson entanglement $S_{\rm sb}$ [colors same as (c)]. Panels (c) and (d) use $N = 6$.

manipulated by, e.g., modulating the confining potential of the ion chain or additional electric fields, to realize single-mode squeezing [23,24,39,40] or a coherent coupling between pairs of modes [25]. The former is described by the unitary operation $\hat{S}(\zeta) = e^{\frac{1}{2}(\zeta^* \hat{a}_m^2 - \zeta \hat{a}_m^{\dagger 2})}$, where $\zeta = re^{i\phi}$ is the squeezing parameter with strength r and phase ϕ. Squeezing reduces the fluctuations along one bosonic quadrature at the expense of increased fluctuations in an orthogonal quadrature. For example, for $\phi = 0$ squeezing transforms $\langle(\Delta\hat{X})^2\rangle = \langle(\hat{X} - \langle\hat{X}\rangle)^2\rangle \to e^{-2r}\langle(\Delta\hat{X})^2\rangle$ and $\langle(\Delta\hat{Y})^2\rangle \to e^{2r}\langle(\Delta\hat{Y})^2\rangle$, where $\hat{X} = \hat{a} + \hat{a}^\dagger$ and $\hat{Y} = i(\hat{a}^\dagger - \hat{a})$. The coherent coupling of phonon modes m and n is described by the unitary operation $\hat{U}_{\rm bs}(\kappa_{mn}) = e^{i\kappa_{mn}(\hat{a}_m^\dagger \hat{a}_n + \hat{a}_n^\dagger \hat{a}_m)/2}$, where setting $\kappa_{mn} = \pi$ realizes a perfect swap of the quantum states of each mode.

Spin-motion coupling can be realized by driving a red sideband transition, described by the (inhomogeneous) Tavis-Cummings Hamiltonian [41–43],

$$H_{{\rm TC},m} = \sum_{j=1}^{N} g_{jm}(\hat{a}_m^\dagger \hat{\sigma}_j^- + \hat{a}_m \hat{\sigma}_j^+). \tag{1}$$

The coupling g_{jm} is determined by the participation of the jth ion in the mth mode. In this work we focus on the center-of-mass (CM) and breathing (B) modes [see Fig. 1(a)]. The former couples uniformly, $g_{jm} = g_0/\sqrt{N}$ with g_0 the characteristic spin-boson coupling strength, while the latter is given by the inhomogeneous coupling $g_{jm} = g_0 u_j / \sqrt{\sum_j u_j^2}$ with u_j the equilibrium position of each ion in the crystal (the origin is chosen to lay at the center of chain) [49].

Noise-reduction protocol.—We first investigate a noise-reduction (NR) protocol [Fig. 1(b)] that generates spin squeezing for a Ramsey sequence. The ions are cooled into the motional ground state of the CM (B) mode and the qubits are prepared uniformly in $|\downarrow\rangle$. The vacuum fluctuations of the CM (B) mode are then squeezed, such that the quadrature variances are $\langle(\Delta\hat{X})^2\rangle = e^{-2r}$ and $\langle(\Delta\hat{Y})^2\rangle = e^{2r}$ with ϕ chosen to be zero. Next, a Tavis-Cummings interaction is applied for a time $t_\pi = \pi/(2g_0)$ [denoted by $\hat{U}_{\rm TC}$ in Fig. 1(b)], ideally leading to a coherent exchange of the fluctuations between the phonons and the spin ensemble [27,50] and thus preparing a squeezed spin state.

Insight into the underlying mechanism can be found in the large N limit by applying a Holstein-Primakoff transformation to the collective raising (lowering) operators, $\sum_{j=1}^N \sigma_j^+ \to \sqrt{N}\hat{b}^\dagger$ ($\sum_{j=1}^N \sigma_j^- \to \sqrt{N}\hat{b}$) [43]. Equation (1) then becomes $\hat{H}_{\rm TC,CM} = g_0(\hat{a}_{\rm CM}^\dagger \hat{b} + \hat{a}_{\rm CM}\hat{b}^\dagger)$, which describes a beam splitter between two bosonic modes. Evolving under $\hat{H}_{\rm TC,CM}$ for t_π thus coherently exchanges the states of the spin and motion. In particular, the collective spin fluctuations after the TC interaction are given by $\langle(\Delta\hat{S}_{y,+})^2\rangle = Ne^{-2r}/4$ and $\langle(\Delta\hat{S}_{x,+})^2\rangle = Ne^{2r}/4$, where $\hat{S}_{\alpha,+} = \frac{1}{2}\sum_{j=1}^N \hat{\sigma}_j^\alpha$ for $\alpha = x, y, z$. Spin squeezing is witnessed by $\xi_s^2 < 1$, where $\xi_s^2 = N\langle(\Delta\hat{S}_{y,+})^2\rangle/|\langle\hat{\mathbf{S}}\rangle|^2$ and $\hat{\mathbf{S}} = (\hat{S}_{x,+}, \hat{S}_{y,+}, \hat{S}_{z,+})$ [26]. More generally, the squeezed spin quadrature can be precisely controlled by varying $\phi \neq 0$ or the phase of the couplings g_{jm}. Similar results are expected for the B mode, though it features squeezed fluctuations of the weighted spin operators $\hat{\mathcal{S}}_\alpha = (\sqrt{N}/2g_0)\sum_{j=1}^N g_{j,{\rm B}}\hat{\sigma}_j^\alpha$ for $\alpha = x, y, z$ such that $\langle(\Delta\hat{\mathcal{S}}_y)^2\rangle \approx Ne^{-2r}/4$ and $\langle(\Delta\hat{\mathcal{S}}_x)^2\rangle \approx Ne^{2r}/4$.

The spin squeezing can subsequently be exploited for metrology using a Ramsey sequence composed of (i) a global $\pi/2$ qubit rotation about $\hat{y}$, (ii) an interrogation period where a phase θ is imprinted by a collective (differential) rotation about $\hat{z}$ described by $\hat{R}_{z,+}^\theta = e^{-i\theta\hat{S}_{z,+}}$ [$\hat{R}_{z,-}^\theta = e^{-i\theta\hat{S}_{z,-}}$ where $\hat{S}_{z,-} = \frac{1}{2}(\sum_{j=1}^{N/2}\hat{\sigma}_j^z - \sum_{j=N/2+1}^N \hat{\sigma}_j^z)$], and (iii) a global $\pi/2$ qubit rotation about $\hat{x}$. The parameter θ is estimated by measuring the spin projections $\hat{M} = \hat{S}_{z,+}$ (CM) and $\hat{M} = \hat{\mathcal{S}}_z$ or $\hat{S}_{z,-}$ (B), with associated sensitivity characterized by the metrological gain $N(\Delta\theta)^2 = N\langle(\Delta\hat{M})^2\rangle/\partial_\theta\langle\hat{M}\rangle|^2$ (equivalent to the spin squeezing ξ_s^2 of the prepared state). Sensitivity surpassing the standard quantum limit corresponds to $N(\Delta\theta)^2 < 1$ with a lower bound $(\Delta\theta)^2 \geq 1/N^2$ given by the Heisenberg limit.

Limitations of the NR protocol.—We assess the role of finite size effects and the inhomogeneous spin-boson couplings for the B mode by numerically simulating the NR protocol and show the results in Figs. 1(b)–1(d). All results are obtained by numerical integration of the Schrödinger equation unless stated otherwise.

Figure 1(c) shows the metrological gain (blue lines) as a function of the boson squeezing $\xi_b^2 = e^{-2r}$ for $N = 6$ qubits. When coupling to the CM mode we find near perfect exchange of fluctuations, $\xi_s^2 \approx \xi_b^2$, for "weak" boson squeezing, before an optimal spin squeezing $\xi_{s,\mathrm{opt}}^2 \approx 3.5$ dB is reached at $\xi_{b,\mathrm{opt}}^2 \approx 5.5$ dB. For $\xi_b^2 < \xi_{b,\mathrm{opt}}^2$ there is an *oversqueezed* regime where spin squeezing is quickly lost. The observation of an optimal $\xi_{s,\mathrm{opt}}^2$ is consistent with the twofold expectations that (i) an ensemble of N qubits can only support a finite amount of squeezing (most stringently, $\xi_s^2 \geq 1/N$), and (ii) the interpretation of the TC interaction as an effective beam splitter is only valid for large N or correspondingly moderate boson squeezing. For both aspects, one should be cognizant that the bosonic fluctuations span a flat 2D phase space defined by the quadratures (X, Y), whereas the spin fluctuations lie on the curved surface of the collective Bloch sphere with axes (S_x, S_y, S_z). The large N limit approximates the spin fluctuations to occupy only the tangential S_x-S_y plane perpendicular to the initial polarization of the spins along $-\hat{z}$. For modest boson squeezing ($\xi_b^2 > \xi_{b,\mathrm{opt}}^2$) this plane is sufficient to describe the squeezed noise exchanged onto the spins, but for large boson squeezing ($\xi_b^2 < \xi_{b,\mathrm{opt}}^2$) it fails as the antisqueezed projection noise probes the curved surface of the Bloch sphere. To illustrate this, we extend our study to larger systems [see Fig. 2(c)] and find that the optimal spin squeezing asymptotically scales as $\xi_{s,\mathrm{opt}}^2 \propto N^{-0.68\pm0.02}$ (uncertainty indicates 95% confidence interval including fitting error) [43]. This is approximately identical to what can be obtained with one-axis twisting [51] and we comment on this shortly.

Similar results are observed for the B mode, although the optimal gain, $N(\Delta\theta)_{\mathrm{opt}}^2 \approx 1.2$ dB at $\xi_{b,\mathrm{opt}}^2 \approx 4.5$ dB, is slightly worse. This is primarily due to $\hat{S}_z$ not quite being the optimal observable to estimate θ, as evidenced by $N(\Delta\theta)^2 > 1$ as $\xi_b^2 \to 1$ [43]. Given that measurement of the weighted spin projection requires detailed knowledge of the couplings $g_{j,\mathrm{B}}$, we also consider the metrological performance for a measurement of the simpler differential magnetization $\hat{S}_{z,-}$, which accounts only for the alternating sign of the B mode coupling across the ion chain [see Fig. 1(a)]. For $N = 6$ this actually leads to slightly superior performance [$N(\Delta\theta)_{\mathrm{opt}}^2 \approx 1.8$ dB]. However, this quickly changes with system size [see Fig. 2(c)] and $\hat{S}_z$ becomes preferable: $N(\Delta\theta)_{\mathrm{opt}}^2 \propto N^{-0.61\pm0.03}$ and $N^{-0.22\pm0.01}$ for the differential and weighted observables, respectively [43].

To further characterize the metrological potential of the prepared probe state we compute the quantum Fisher information (QFI) $F_Q = 4\langle(\Delta\hat{S}_{x,\pm})^2\rangle$, which constrains

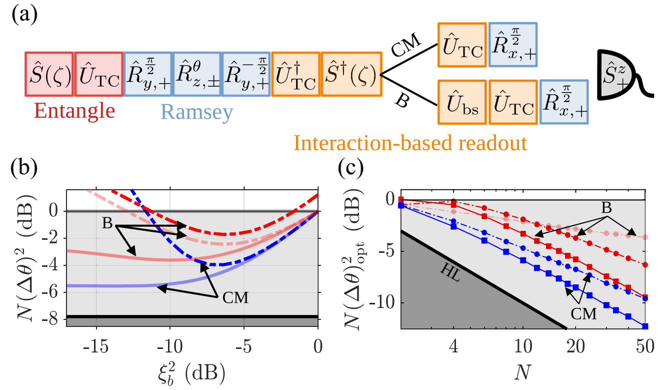

FIG. 2. (a) Sequence for SA protocol. The final steps of the IBR depend on the coupled mode and measurement. (b) Metrological gain as a function of boson squeezing ξ_b^2 using $\hat{M} = \hat{S}_{z,+}$ (CM and B, dot-dashed blue and red lines) and $\hat{S}_{z,-}$ (B, faded dot-dashed red line). We also plot the QCRB N/F_Q (faded blue and red lines). Calculations use $N = 6$. (c) Scaling of optimal metrological gain with ion number N for NR (circles) and SA (squares) protocols for the CM (blue) and B (red) modes. We distinguish $\hat{S}_{z,-}$ (faded) and $\hat{S}_z$ (darker) measurements for the B mode NR protocol. Data for this panel is obtained using a truncated Wigner approximation [43,52].

the best sensitivity (optimized over all measurements) by the quantum Cramer-Rao bound (QCRB) $(\Delta\theta)^2 \geq F_Q^{-1}$. We plot the optimal metrological gain NF_Q^{-1} in both panels of Fig. 1(c) (red lines). The QFI predicts a significantly enhanced metrological gain relative to spin squeezing for $\xi_b^2 < \xi_{b,\mathrm{opt}}^2$ and saturates to $NF_Q^{-1} \approx N/2$ for large boson squeezing.

The *oversqueezed* regime featuring large QFI but poor squeezing as a result of the curved Bloch sphere is reminiscent of one-axis twisting protocols in collective spin systems [34,51]. For these, measurements of higher-order observables [53,54] or counting statistics [17,55] can be used to approach the QCRB. In contrast, oversqueezing in our protocol is associated with spin-boson entanglement. Figure 1(d) shows the Renyi entanglement entropy $S_{\mathrm{sb}} = -\log[\mathrm{Tr}(\hat{\rho}_s^2)]$, where $\hat{\rho}_s = \mathrm{Tr}_{\mathrm{ph}}[\hat{\rho}]$ is the reduced density matrix of the spins. While S_{sb} is vanishingly small in the squeezed regime ($\xi_b^2 > \xi_{b,\mathrm{opt}}^2$), it grows appreciably in the oversqueezed regime ($\xi_b^2 < \xi_{b,\mathrm{opt}}^2$) and the entanglement leads to excess projection noise in the reduced spin subsystem (as it becomes mixed), thereby limiting the sensitivity attainable with spin measurements. For the CM case, we illustrate this by a calculation of the QFI of the spin subsystem, $F_{Q,s}(\rho_s)$ [43] [magenta dotted line in panel (b)], satisfying $F_{Q,s} \leq F_Q$ and quantifying the metrological potential of the prepared state when constrained to spin measurements. We observe that $NF_{Q,s}^{-1}$ is appreciably worse than NF_Q^{-1} in the oversqueezed regime, implying that joint measurements of the spins and bosons are required to saturate the QCRB.

Signal amplification protocol.—To exploit the oversqueezed regime we propose a signal amplification (SA) protocol based on IBR. An example sequence is shown in Fig. 2(a): We supplement the NR protocol by a time-reversal sequence where the TC interaction and boson squeezing operation are undone (achieved by flipping the sign of the respective Hamiltonian through single qubit manipulations and/or jumping the phase of applied lasers and electric fields) and a final mode-dependent readout step.

In the large N limit, the time-reversal sequence maps the rotation of the complex, entangled probe state to a simple, disentangled product state. Specifically, undoing the TC interaction transforms the spin rotation into an effective coherent displacement of the phonon mode, $\hat{U}_{\rm TC}\hat{R}^{(\pi/2)}_{y,+}\hat{R}^{\theta}_{z,\pm}\hat{R}^{(\pi/2)}_{y,+}\hat{U}^{\dagger}_{\rm TC} \equiv \hat{D}(\sqrt{N}\theta)$, where $\hat{D}(\alpha) = e^{i\alpha\hat{Y}}$. This displacement is amplified by the squeezing-unsqueezing of the phonon mode according to $\hat{S}^{\dagger}(\zeta)\hat{D}(\sqrt{N}\theta)\hat{S}(\zeta) \equiv \hat{D}(e^{r}\sqrt{N}\theta)$ [23,40,56]. After time reversal, θ is encoded solely in the displacement of the phonon mode, which is typically not amenable to direct detection. Thus, we use an additional TC interaction to transform the phonon displacement to a rotation of the spin ensemble by an angle $e^{r}\theta$ about $-\hat{z}$, which can be characterized by, e.g., a simple measurement of the collective magnetization via fluorescence.

The protocol for the B mode is understood analogously, with the final TC interaction followed by a measurement of $\hat{\mathcal{S}}_z$ or $\hat{S}_{z,-}$. However, one could also add a beam-splitter operation $\hat{U}_{\rm bs}$ that couples the CM and B modes after the time-reversal sequence [25] [see lower sequence in Fig. 2(a)], which interchanges the state of the displaced B mode with the unused CM mode. The rotation angle θ is inferred from the collective magnetization after a final TC interaction. This alternative sequence enables sensing of differential rotations with no requirement for single-ion resolution or manipulation.

Figure 2(b) shows the metrological gain achieved with the SA protocol as a function of boson squeezing for an example of $N = 6$ ions. For the B mode, the same gain is obtained whether $\hat{\mathcal{S}}_z$ or $\hat{S}_{z,+}$ (after the coupling of the CM and B modes) is measured and thus we only plot the former in Figs. 2(b) and 2(c). We find the optimal metrological gain is $N(\Delta\theta)^2_{\rm opt} = 4$ dB and 2 dB for $\xi_b^2 \approx 6$ dB using the CM and B modes, respectively. Additionally, we find $F_{Q,s} = F_Q$ for all ξ_b^2 (see Ref. [43]) and point out that the QCRB (faded blue and red lines in Fig. 2(b)) could be saturated by a more demanding measurement of the projection onto the initial spin state [57,58] or spin counting statistics [43]. The enhancement provided by the SA protocol is emphasized with increasing system size. Figure 2(c) shows the optimal metrological gain as a function of N and we find $N(\Delta\theta)^2_{\rm opt} \propto N^{-0.87\pm0.03}$ and $N^{-0.77\pm0.06}$ for coupling to the CM and B modes, respectively [43].

Decoherence and noise.—Various technical factors contribute to the performance of our protocols in practice. Imperfect cooling of the targeted normal mode leads to a thermal occupation of $\bar{n}$ phonons and thus excess motional fluctuations before squeezing is applied. This excess noise is inherited by the spin ensemble and also exacerbates finite size effects during the TC interaction. Overall, we predict a degradation in the metrological gain by a factor of $(2\bar{n}+1)^2$ relative to the ideal case [43]. State-of-the-art trapped ion experiments routinely cool normal modes to near vacuum ($\bar{n} \ll 1$) [59–61].

Damping or heating of the normal modes at a characteristic rate κ during the protocols can have two relevant effects. First, we require $g_0 \gg \kappa$ so that the TC interaction is much faster than the relevant motional decoherence, which would otherwise degrade the squeezing transferred to the spin state and the efficacy of the IBR. Simultaneously, g_0 (and thus κ) should be small compared to the relevant frequency spacing of the normal modes near the CM or B modes, so that Eq. (1) is valid. This may be a consideration for larger 1D chains with closely spaced axial modes but we emphasize that our proposal can be extended to radial modes or higher-dimensional arrays. Secondly, the SA protocol may be sensitive to motional decoherence during long phase interrogation periods if operating with states featuring spin-boson entanglement. Spin decoherence can also be relevant, although our protocol occurs on a fixed timescale set by $t_\pi = 2\pi/g_0$, whereas squeezing via spin-spin interactions can be more susceptible to decoherence due to intrinsically slower timescales that increase with system size [16,17,43]. In addition, the impact of off-resonant light scattering on the sideband protocols that we discuss can scale more favorably with the detuning from relevant internal states than protocols based on spin-spin interactions [43,62].

A lack of phase coherence between the independent fields driving the bosonic squeezing and spin-motion coupling lead to effective shot-to-shot fluctuations of the squeezing angle ϕ [43]. In the large N limit, the NR protocol with the CM mode is limited to $N(\Delta\theta)^2_{\rm opt} \approx 2\sigma$, where $\sigma \ll 1$ is the rms fluctuation of the squeezing angle, and squeezing is lost entirely for $\sigma \gg 1$. In contrast, the SA protocol yields $N(\Delta\theta)^2 \approx e^{-2r}(1+2\sigma^2)$ for $\sigma \ll 1$ and $N(\Delta\theta)^2 \approx 4e^{-2r}$ for $\sigma \gg 1$ [43]. Thus, we only require

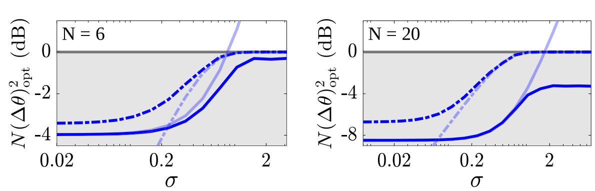

FIG. 3. Optimal metrological gain as a function of phase noise magnitude σ for NR (dot-dashed lines) and SA (solid lines) protocols with $N = 6$ and $N = 20$ for CM mode. Faded lines are approximate analytic predictions [43].

independent stability of the boson and spin operations to retain a quantum enhancement. Numerical calculations for $N = 6$ and $N = 20$ ions are shown in Fig. 3. While finite size effects are stronger in the former case, our results are still qualitatively consistent with the large N predictions. Similar robustness is found for the B mode [43].

Summary and outlook.—Our work suggests new opportunities for many-body state preparation and sensing with trapped ions by exploiting the available control over both spin and motion. Arrays in 2D and 3D can provide further diversity of normal modes for preparing spin states with complex spatially structured correlations, while bespoke modes can be created by trapping multiple species [63] or additional tweezer potentials [64]. Our results complement recent studies of multiparameter estimation in collective spin systems [3–5,9,65], with the distinction that by exploiting the natural structure of collective motion in ion crystals we only require global control and imaging of the qubits.

We acknowledge stimulating discussions with J. J. Bollinger, D. T. C. Allcock, and A. L. Carter. R. J. L.-S. and J. Z. acknowledge support by NSF through Grant No. PHY-2110052 and by the U.S. Department of Energy, Office of Science, Advanced Scientific Computing Research, Exploratory Research for Extreme-Scale Science program. A. M. R. and D. B. acknowledge support from ARO W911NF-19-1-0210, NSF JILA-PFC PHY-2317149, NSF QLCI-2016244, the DOE Quantum Systems Accelerator (QSA) grant, The Simons Foundation, the Vannevar Bush Faculty Fellowship (VBFF) and by NIST. A. M. R. and D. B. acknowledge support from ARO W911NF-19-1-0210, NSF JILA-PFC PHY-2317149, NSF QLCI-2016244, the DOE Quantum Systems Accelerator (QSA) grant, The Simons Foundation, and by NIST. The computing for this project was performed at the OU Supercomputing Center for Education & Research (OSCER) at the University of Oklahoma (OU).

[1] L. Pezzè, A. Smerzi, M. K. Oberthaler, R. Schmied, and P. Treutlein, Rev. Mod. Phys. **90**, 035005 (2018).
[2] S. S. Szigeti, O. Hosten, and S. A. Haine, Appl. Phys. Lett. **118**, 140501 (2021).
[3] Y. Jing, M. Fadel, V. Ivannikov, and T. Byrnes, New J. Phys. **21**, 093038 (2019).
[4] M. Gessner, A. Smerzi, and L. Pezzè, Nat. Commun. **11**, 3817 (2020).
[5] M. Fadel, B. Yadin, Y. Mao, T. Byrnes, and M. Gessner, New J. Phys. **25**, 073006 (2023).
[6] B. K. Malia, Y. Wu, J. Martínez-Rincón, and M. A. Kasevich, Nature (London) **612**, 661 (2022).
[7] E. S. Cooper, P. Kunkel, A. Periwal, and M. Schleier-Smith, arXiv:2212.11961.
[8] R. Kaubruegger, A. Shankar, D. V. Vasilyev, and P. Zoller, PRX Quantum **4**, 020333 (2023).
[9] Y. Baamara, M. Gessner, and A. Sinatra, SciPost Phys. **14**, 050 (2023).
[10] J. Czartowski, K. Życzkowski, and D. Braun, arXiv:2303.08591.
[11] J. W. Britton, B. C. Sawyer, A. C. Keith, C.-C. J. Wang, J. K. Freericks, H. Uys, M. J. Biercuk, and J. J. Bollinger, Nature (London) **484**, 489 (2012).
[12] C. Monroe, W. C. Campbell, L.-M. Duan, Z.-X. Gong, A. V. Gorshkov, P. W. Hess, R. Islam, K. Kim, N. M. Linke, G. Pagano, P. Richerme, C. Senko, and N. Y. Yao, Rev. Mod. Phys. **93**, 025001 (2021).
[13] M. A. Norcia, R. J. Lewis-Swan, J. R. K. Cline, B. Zhu, A. M. Rey, and J. K. Thompson, Science **361**, 259 (2018).
[14] E. J. Davis, G. Bentsen, L. Homeier, T. Li, and M. H. Schleier-Smith, Phys. Rev. Lett. **122**, 010405 (2019).
[15] I. D. Leroux, M. H. Schleier-Smith, and V. Vuletić, Phys. Rev. Lett. **104**, 073602 (2010).
[16] J. Franke, S. R. Muleady, R. Kaubruegger, F. Kranzl, R. Blatt, A. M. Rey, M. K. Joshi, and C. F. Roos, Nature (London) **621**, 740 (2023).
[17] J. G. Bohnet, B. C. Sawyer, J. W. Britton, M. L. Wall, A. M. Rey, M. Foss-Feig, and J. J. Bollinger, Science **352**, 1297 (2016).
[18] D. M. Meekhof, C. Monroe, B. E. King, W. M. Itano, and D. J. Wineland, Phys. Rev. Lett. **76**, 1796 (1996).
[19] C. Monroe, D. M. Meekhof, B. E. King, and D. J. Wineland, Science **272**, 1131 (1996).
[20] P. O. Schmidt, T. Rosenband, C. Langer, W. M. Itano, J. C. Bergquist, and D. J. Wineland, Science **309**, 749 (2005).
[21] H. Häffner, C. Roos, and R. Blatt, Phys. Rep. **469**, 155 (2008).
[22] C. Flühmann, T. L. Nguyen, M. Marinelli, V. Negnevitsky, K. Mehta, and J. P. Home, Nature (London) **566**, 513 (2019).
[23] S. C. Burd, R. Srinivas, J. J. Bollinger, A. C. Wilson, D. J. Wineland, D. Leibfried, D. H. Slichter, and D. T. C. Allcock, Science **364**, 1163 (2019).
[24] S. C. Burd, R. Srinivas, H. M. Knaack, W. Ge, A. C. Wilson, D. J. Wineland, D. Leibfried, J. J. Bollinger, D. T. C. Allcock, and D. H. Slichter, Nat. Phys. **17**, 898 (2021).
[25] P. Hou, J. Wu, S. Erickson, D. Cole, G. Zarantonello, A. Brandt, A. Wilson, D. Slichter, and D. Leibfried, arXiv:2205.14841.
[26] D. J. Wineland, J. J. Bollinger, W. M. Itano, F. L. Moore, and D. J. Heinzen, Phys. Rev. A **46**, R6797 (1992).
[27] D. J. Wineland, J. J. Bollinger, W. M. Itano, and D. J. Heinzen, Phys. Rev. A **50**, 67 (1994).
[28] A. Kuzmich, K. Mølmer, and E. S. Polzik, Phys. Rev. Lett. **79**, 4782 (1997).
[29] J. Hald, J. L. Sørensen, C. Schori, and E. S. Polzik, Phys. Rev. Lett. **83**, 1319 (1999).
[30] B. Sundar, D. Barberena, A. P. n. Orioli, A. Chu, J. K. Thompson, A. M. Rey, and R. J. Lewis-Swan, Phys. Rev. Lett. **130**, 113202 (2023).
[31] J. M. Robinson, M. Miklos, Y. M. Tso, C. J. Kennedy, T. Bothwell, D. Kedar, J. K. Thompson, and J. Ye, Nat. Phys. **20**, 208 (2024).
[32] T. Bothwell, C. J. Kennedy, A. Aeppli, D. Kedar, J. M. Robinson, E. Oelker, A. Staron, and J. Ye, Nature (London) **602**, 420 (2022).

[33] T. Ruster, H. Kaufmann, M. A. Luda, V. Kaushal, C. T. Schmiegelow, F. Schmidt-Kaler, and U. G. Poschinger, Phys. Rev. X **7**, 031050 (2017).
[34] E. Davis, G. Bentsen, and M. Schleier-Smith, Phys. Rev. Lett. **116**, 053601 (2016).
[35] S. P. Nolan, S. S. Szigeti, and S. A. Haine, Phys. Rev. Lett. **119**, 193601 (2017).
[36] K. A. Gilmore, M. Affolter, R. J. Lewis-Swan, D. Barberena, E. Jordan, A. M. Rey, and J. J. Bollinger, Science **373**, 673 (2021).
[37] S. Colombo, E. Pedrozo-Peñafiel, A. F. Adiyatullin, Z. Li, E. Mendez, C. Shu, and V. Vuletić, Nat. Phys. **18**, 925 (2022).
[38] G. S. Agarwal and L. Davidovich, Phys. Rev. Res. **4**, L012014 (2022).
[39] D. J. Heinzen and D. J. Wineland, Phys. Rev. A **42**, 2977 (1990).
[40] W. Ge, B. C. Sawyer, J. W. Britton, K. Jacobs, J. J. Bollinger, and M. Foss-Feig, Phys. Rev. Lett. **122**, 030501 (2019).
[41] C. E. López, F. Lastra, G. Romero, and J. C. Retamal, Phys. Rev. A **75**, 022107 (2007).
[42] A. Retzker, E. Solano, and B. Reznik, Phys. Rev. A **75**, 022312 (2007).
[43] See Supplemental Material at http://link.aps.org/supplemental/10.1103/PhysRevLett.132.163601 for additional theoretical calculations and discussion, which includes Refs. [44–48].
[44] T. Holstein and H. Primakoff, Phys. Rev. **58**, 1098 (1940).
[45] J. J. Bollinger, W. M. Itano, D. J. Wineland, and D. J. Heinzen, Phys. Rev. A **54**, R4649 (1996).
[46] S. C. Burd, H. M. Knaack, R. Srinivas, C. Arenz, A. L. Collopy, L. J. Stephenson, A. C. Wilson, D. J. Wineland, D. Leibfried, J. J. Bollinger, D. T. C. Allcock, and D. H. Slichter, arXiv:2304.05529.
[47] J. W. Britton, B. C. Sawyer, A. C. Keith, C.-C. J. Wang, J. K. Freericks, H. Uys, M. J. Biercuk, and J. J. Bollinger, Nature (London) **484**, 489 (2012).
[48] R. J. Lewis-Swan, M. A. Norcia, J. R. K. Cline, J. K. Thompson, and A. M. Rey, Phys. Rev. Lett. **121**, 070403 (2018).
[49] D. F. V. James, Appl. Phys. B **66**, 181 (1998).
[50] X. Wang and B. C. Sanders, Phys. Rev. A **68**, 033821 (2003).
[51] M. Kitagawa and M. Ueda, Phys. Rev. A **47**, 5138 (1993).
[52] A. Piñeiro Orioli, A. Safavi-Naini, M. L. Wall, and A. M. Rey, Phys. Rev. A **96**, 033607 (2017).
[53] M. Gessner, A. Smerzi, and L. Pezzè, Phys. Rev. Lett. **122**, 090503 (2019).
[54] Y. Baamara, A. Sinatra, and M. Gessner, C.R. Phys. **23**, 1 (2022).
[55] H. Strobel, W. Muessel, D. Linnemann, T. Zibold, D. B. Hume, L. Pezze, A. Smerzi, and M. K. Oberthaler, Science **345**, 424 (2014).
[56] W. Ge, B. C. Sawyer, J. W. Britton, K. Jacobs, M. Foss-Feig, and J. J. Bollinger, Phys. Rev. A **100**, 043417 (2019).
[57] T. Macrì, A. Smerzi, and L. Pezzè, Phys. Rev. A **94**, 010102(R) (2016).
[58] M. Gärttner, J. G. Bohnet, M. Safavi-Naini, M. L. Wall, J. J. Bollinger, and A. M. Rey, Nat. Phys. **13**, 781 (2017).
[59] E. Jordan, K. A. Gilmore, A. Shankar, A. Safavi-Naini, J. G. Bohnet, M. J. Holland, and J. J. Bollinger, Phys. Rev. Lett. **122**, 053603 (2019).
[60] L. Feng, W. L. Tan, A. De, A. Menon, A. Chu, G. Pagano, and C. Monroe, Phys. Rev. Lett. **125**, 053001 (2020).
[61] D. Kiesenhofer, H. Hainzer, A. Zhdanov, P. C. Holz, M. Bock, T. Ollikainen, and C. F. Roos, PRX Quantum **4**, 020317 (2023).
[62] A. L. Carter, S. R. Muleady, A. Shankar, J. F. Lilieholm, B. B. Bullock, M. Affolter, A. M. Rey, and J. J. Bollinger, Phys. Rev. A **107**, 042618 (2023).
[63] K. Sosnova, A. Carter, and C. Monroe, Phys. Rev. A **103**, 012610 (2021).
[64] M. Mazzanti, R. X. Schüssler, J. D. Arias Espinoza, Z. Wu, R. Gerritsma, and A. Safavi-Naini, Phys. Rev. Lett. **127**, 260502 (2021).
[65] R. Kaubruegger, A. Shankar, D. V. Vasilyev, and P. Zoller, PRX Quantum **4**, 020333 (2023).